

**MODELLING OF CELL SUSPENSION
DURING CRYOPRESERVATION**

Krishna Reddy

MODELLING OF CELL SUSPENSION DURING CRYOPRESERVATION

*Thesis submitted to the
National Institute of Technology, Rourkela
for the award of the degree*

of

Master's of Technology in Biotechnology

by

Krishna Reddy

Under the guidance of

Dr. Amitesh Kumar



DEPARTMENT OF BIOTECHNOLOGY & MEDICAL ENGINEERING

NATIONAL INSTITUTE OF TECHNOLOGY, ROURKELA

JUNE 2013

©2013 Krishna Reddy. All rights reserved.

CERTIFICATE

This is to certify that the thesis entitled **Modelling Of Cell Suspension During Cryopreservation**, submitted by **Krishna Reddy** to National Institute of Technology, Rourkela, is a record of bona fide research work under my supervision and I consider it worthy of consideration for the award of the degree of Master's of Technology of the Institute.

Date :

Dr. Amitesh Kumar
Assistant Professor
Department of Biotechnology & Medical
Engineering
National Institute of Technology
Rourkela, 769008

DECLARATION

I certify that

1. The work contained in the thesis is original and has been done by myself under the general supervision of my supervisor.
2. The work has not been submitted to any other Institute for any degree or diploma.
3. I have followed the guidelines provided by the Institute in writing the thesis.
4. I have conformed to the norms and guidelines given in the Ethical Code of Conduct of the Institute.
5. Whenever I have used materials (data, theoretical analysis, and text) from other sources, I have given due credit to them by citing them in the text of the thesis and giving their details in the references.

Krishna Reddy

ACKNOWLEDGEMENTS

I am deeply grateful to my supervisor, Dr. Amitesh Kumar, whose insights and encouragements have contributed so much to this thesis. No words are enough to express my gratitude to my mentor for his whole hearted, unflinching encouragement, meticulous supervision and support. He would take a great concern in troubleshooting problems and was always full of encouraging words. His words of applause and sincere criticism in the last one year helped me a lot to develop my ideas regarding many important issues in life.

I would like to thank all of my colleagues and friends for their inspiration and help.

I would like to thank my parents for their encouragement, love and friendship.

At last, I would like to express my deep sense of gratitude to almighty GOD, many known and unknown hands which pushed me forward.

Date :

Place :

Krishna Reddy

Contents

Certificate	i
Declaration	iii
Acknowledgements	v
Contents	vii
List of Figures	ix
List of Symbols and Abbreviations	xi
Abstract	xiii
1 INTRODUCTION	1
1.1 Introduction	1
1.2 Literature Review	5
1.3 Objective	7
2 Mathematical Modelling	9
2.1 Overview of Solidification Phenomena	9
2.2 Solidification of a Pure Liquid	9
2.3 Freezing of a Binary Solution	11
2.4 Freezing of water sodium chloride solution	15
2.5 Mathematical Model of Water Transport	15
2.6 Numerical Simulations	18
3 Results & Discussion	21
3.1 Temperature and Concentration distribution in cryovial	21
3.2 Kinetics of Cell Water Loss at Different Locations in the Cryovial	27
3.3 Survivability	30
3.4 Conclusion	32

Bibliography

33

List of Figures

2.1	Schematic model of phase change heat transfer of a pure substance: (a) freezing and (b) thawing.	10
2.2	Equilibrium phase diagram for a fictitious binary system X–Y.	12
2.3	Equilibrium phase diagram of aqueous sodium chloride solution [1].	15
2.4	Schematic diagram of cryovial and coordinate system.	18
3.1	Solute concentration distribution in the solution during freezing of 5% weight at a different cooling conditions.	22
3.2	Temperature profiles in the solution during freezing of 5% weight at a different cooling conditions.	24
3.3	Solute concentration distribution in the solution during freezing of 10% weight of a different cooling conditions.	25
3.4	Temperature profiles in the solution during freezing of 10% weight at a different cooling conditions.	26
3.5	Intracellular water volume variation with time during freezing of model cells at different locations in the cryovial under boundary cooling conditions and solute concentration 5%.	28
3.6	Intracellular water volume variation with time during freezing of model cells at different locations in the cryovial under boundary cooling conditions and solute concentration 10%.	29
3.7	Relation of cell viability to cooling temperatures with initial solution concentrations 5% and 10%	31

LIST OF SYMBOLS AND ABBREVIATIONS

L_{pg}	Reference Membrane Permeability ($\mu\text{m}/\text{min-atm}$)
L_p	Plasma Membrane Permeability ($\mu\text{m}/\text{min-atm}$)
E_{Lp}	Activation Energy (Kcal/mole)
SA	Surface Area
V_b	Initial Water Volume
V	Cell Volume
V_o	Isotonic or Initial Cell Volume
c_p	specific heat (J/kg K)
T_{end}	End Temperature at which Water Transport Ceases
T	Absolute Temperature (K)
T_R	Reference Temperature (273.15K)
A_c	Effective Membrane Surface Area Available for Water Transport
v_w	Molar Volume of Water ($18 \times 10^{-6} \text{m}^3/\text{mole}$)
a_w^o	Chemical Potential of Extracellular Fluid
H	specific total enthalpy (J/kg)
a_w^i	Chemical Potential of Intracellular Fluid
R	Gas Constant ($8.02 \times 10^{-2} \text{m}^3\text{-atm}/\text{mol K}$)
h	specific sensible enthalpy (J/kg)
ΔH_f	Latent Heat of Fusion of Water (335 J/gm)
C_i	Initial Cell Osmolality (0.285)
φ_s	Dissociation Constant for NaCl (=2)
n_s	Number of Moles of Solutes in the Cell ($C_i (V_o - V_b)$)
ρ	Density of Water (1000 kg/m ³)
D	Ddiffusion coefficient
k	thermal conductivity (W/m K)
g	solid volume fraction
T	temperature (K)
t	time (s)

Dimensionless Numbers

r/r_0	Normalised distance
V/V_0	Normalised cell volume
Ste	Stefan number

Greek Letters

α, β	Solid phases of different composition
ρ	density of the solution (kg/m ³)

Subscript

∞	ambient condition
E	eutectic

<i>l</i>	liquidus
<i>m</i>	melting
max	maximum value
<i>s</i>	solidus

Superscript

*	dimensionless
'	per unit length

ABSTRACT

In the present study, One-dimensional numerical model for cryopreservation is developed to design a mathematical model that allows prediction of the transient temperature and solute concentration distributions and corresponding cell responses at any location (in the solidified, mushy, and liquid regions) in a cell suspension during cooling processes. The continuum model for binary component phase change system is considered for simulating the freezing process of binary solution ($H_2O-NaCl$). The formalism is extended to the freezing of a cell solution. An implicit scheme for coupling temperature and concentration fields in solidification model is employed. Mathematical predictions of the un-steady state temperature profile, mushy region and eutectic composition are obtained and then using the temperature and salt concentration data, the kinetics of water loss and survivability of model cell are predicted. The equine sperms is modeled as a cylinder of length $36.5 \mu m$ and radius of $0.66 \mu m$ with an osmotically inactive cell volume (V_b) of $0.6V_0$, where V_0 is the isotonic cell volume. The volumetric shrinkage during freezing of equine sperm suspensions at holding temperature between $-20^{\circ}C$ and $-50^{\circ}C$ in the absence of cryoprotective agents (CPAs) for different initial solute concentrations of 5% and 10% is predicted. The percentage of viable equine sperm was 13% and 8% at holding temperature of $-38^{\circ}C$ and $-25^{\circ}C$ for initial solute concentration of 5% and 10% respectively. Sperm viability is found to be almost constant between $-25^{\circ}C$ and $-40^{\circ}C$ for an initial solute concentration of 10%.

Keywords: Cryopreservation, Solidification, Finite volume method.

CHAPTER 1

INTRODUCTION

1.1 Introduction

Cryobiology is the division of science, which deals with the effects of decreased temperatures on living organisms, their essential parts, and their products. One important goal of the arena of cryobiology is to preserve and store viable biological cells or organisms in the frozen state for long periods of time in order to confirm reproducible results and continuity and implement in research and biomedical developments. One such technique to preserve and stabilize genetically of the biological systems is the “cryopreservation” process. Cryopreservation refers to the preserving of a living organism at extreme low temperature in suspended liveliness for lengthier periods of time, such that it can be recovered and returned to the same living state as before it was preserved. Developments in cryopreservation tools have made it possible to improve new methods that permit reduced temperature preservation of a variety of cells and organisms and tissues. Cryopreservation tools are developed for the preservation of various biological materials such as, isolated tissue cells, microorganisms, small multicellular biological systems and even more complex organisms such as embryos. These techniques have been effectively applied to a variety of mammalian biological systems such as lymphocytes, red blood cells, granulocytes, platelets, gametes and embryos, pancreatic tissue, bone marrow stem cells, hepatocytes, cornea and skin, kidney and heart, etc. as revised by [2]and [3]. Other perspectives of applied cryobiology that are of importance include the preservation of food freezing, human and non-human mammalian oocytes [4], tissue engineered equivalents [5], parasites and protozoa, fish, insects, plants including algae and microorganisms. Other purposes include cryopreservation of human

and rat liver slices [6], aquatic species and fish gametes and spermatozoa from diversity of species, including human sperm [7] and equine sperm [8].

The freezing process involves a complicated event that, even after years of research, are not fully comprehended. Water is the chief component of all active cells and it must be accessible for all the chemical processes of life to happen and cellular metabolism halts when all the water in the system is transformed to ice. As the cell water is considered indispensable to the structure and efficient performance of living cells, therefore, the state of the water plays an essential role in cell survival throughout a freezing process. It's significant to understand, qualitatively and quantitatively, what occurs to this cell water as the cells are exposed to freezing temperatures. Ice tends to appear at different rates during a freezing process. As the cell in solution is subjected to a freezing procedure, ice first forms in the extracellular space. The cell membrane precludes the formation of ice inside the cell and as a consequence the intracellular solution becomes super cooled. Due to the occurrence that the partly frozen extracellular solution has a inferior chemical potential than the unfrozen super cooled intracellular solution, a chemical potential difference is established around the cell membrane [9]. This effects in a thermodynamically non-equilibrium state that stipulates a driving force for the two biophysical processes during freezing, cellular dehydration or the loss of intracellular water and the creation of intracellular ice [2]. At low cooling rates cellular dehydration is the central mechanism whereas at very rapid cooling rates intracellular ice formation (IIF) is the dominant mechanism [10]. Both cellular dehydration and IIF have been shown to be venomous to the post-thaw survival of biological systems [11], [12]. The rate of cooling has a theatrical effect on these two biophysical processes. If the cooling rate is sufficiently slow, there will be adequate time for the cell water to leave the cell and join the extracellular space. The result is the cell loses water swiftly by exmosis to concentrate the intracellular liquid necessarily enough to abolish super cooling and maintain chemical potential of intracellular water in equilibrium with that of extracellular water. The resulting changes in the extracellular area, such as changes in pH, changes in ionic concentration cause the tertiary structure of proteins to unfold, so that some of its unique properties, especially its biological activity, are reduced or eliminated. This denaturation of cell proteins may be mortal to cell survival [11]. In adding, mechanical interaction between extracellular ice crystals and cells can also lead to the deformation of cells and breach of cell membranes [13]. On the other hand if the cell is cooled too rapidly it is not capable to lose water fast enough to get equilibrium; it becomes increasingly super cooled and in the end attains equilibrium by freezing intracellularly. Intracellular ice formation (IIF) is generally lethal as it affects injury to cellular membranes and intracellular structures. So, cooling velocities which are either "too slow" or "too fast" can and do decrease the post thaw survival of the cells, thus, a cooling rate for maximum cell cryosurvival should and does exist between the "high" and "low" rates [3]. This has

been proved experimentally for a variety of cells and the curve of cell survival plotted as a function of the cooling rate, has a characteristic U- shape [12]. Permeability of the membrane shows how fast the water can leave the cell at a given cooling rate. More the permeability of the membrane, more the water transport across the cell membrane in a given time and vice versa. Hence, whether a prescribed cooling rate is too “slow” or too “fast,” is a function of cell membrane permeability to water and the probability that any water remaining trapped within the cell at any given subzero temperature will nucleate and converted into ice. The variance in membrane permeability to water and probability of IIF results in distinctive optimal cooling rates for different cells. Therefore, to find out the optimal cooling rate for most cell survival and to optimize a cryopreservation protocol, it is essential to measure the cell membrane’s permeability to water. Evidently, the quantitative understanding of the water transport across the cell membrane during a cryopreservation is critical for the accomplishment of the respective protocol.

The background of this study is the cryopreservation of biological cells suspended in aqueous media particularly in a so-called, isotonic, i.e. physiological, solution of sodium chloride in water ($C_0 = 0.1548 \text{ mol}^{-1}$). In the case of Equine spermcells, such suspension is commonly frozen in cryovial or straws containers by exposing the whole arrangement to a liquid nitrogen cooling device. In this way solidification is initiated in the suspending medium. Due to the variation of composition in the residual liquid during solidification, biological cells can react by an efflux of intracellular substances, whose amount is a pivotal quantity for their survival in the whole freezing process. To establish the maximum probability of survival, it is needed to gain complete knowledge of the freezing behaviour of the suspending medium (i.e. isotonic solution of NaCl in water). At such low temperatures, physiological processes are slowed or suspended, and thus the phenomena of prominence are reduced to physical transport of heat, water and solute. The primary factors controlling cell response to freezing are the cooling rate and temperatures imposed on the cell. Thermodynamics of aqueous solutions precepts that when a solution is cooled ice will precipitate out leaving the remaining solution more concentrated in solute (salts such as NaCl in the human cell and surrounding tissue [14], as given by the phase diagram of the mixture. Therefore, suppose that the cell is initially suspended in an isotonic solution (i.e. the salt concentration in the cell and the surrounding medium are equal). When the mixture is cooled, due to thermodynamic effects [15], ice will first form in the extracellular solution. As the extracellular ice crystals grow, the cell finds itself in surroundings with increasing solute concentration (i.e. in a hypertonic medium). This non-equilibrium condition drives water molecules out of the cell (exosmosis) through the semi-permeable cell membrane [14], thus shrinking (dehydrating) the cell. The key to cell survival is the rate at which cooling is done. If cooling is too rapid, water molecules cannot leave the cell at a rapid enough rate; as the temperature drops ice begins to form inside the cell. Thus, the intracellular ice formation

(IIF) mechanism [2] of cell death is impending. Intracellular ice crystals impair the cell and it will not survive the freeze-thaw process. If the cooling is too slow, then water will leave the cell too gradually, so that the cell will find itself in an increasingly hypertonic environment for longer durations, which again risks the cell. This is death due to “solution effects” [9]. Cell death can be delayed/ prohibited by controlling the two effects, i.e. rate of water loss from the cell and increase in the concentration of solute (tonicity) of the surrounding medium. Since 1963, different theoretical models and equations have been developed to explain the cell response (e.g., probability of intracellular ice nucleation and intracellular water loss, water flux across cell membrane) to the environmental change during the freezing and thawing processes [16]. Using these models, optimum holding temperature or optimal cooling rate have been successfully predicted to prevent cryoinjury to some cell types. However, these models were started/ established based on a basic assumption that the solute concentration and temperature distributions are uniform in the cryopreserved cell suspensions or tissues during the freezing or solidification of biological solution and thawing processes [2]. Under this assumption, the cell’s response to the local environmental variation is the similar everywhere in a sample (either a cell suspension or tissue). This assumption becomes challenging particularly if cryopreserved samples are comparatively large in dimension, because biological systems have low thermal conductivity and high thermal capacity. The time reliant temperature and solute concentration distributions are non-uniform in these samples during cooling and warming processes. Determination of the temperature and solute concentration distributions as well as phase change state is essential for predicting cell behaviour in response to local environmental changes and for designing optimum cryopreservation conditions. An understanding of the mechanism of solution effects injury depends upon an understanding of the compositional changes brought about in the extracellular solution during the freezing process. Mathematical modelling [17] of momentum, mass, heat, and species transport phenomena during solidification of binary and multicomponent solutions has been developed. Emphasis is placed on the interactions between the solid and liquid phases on a microscopic scale into a (macroscopic) model of the transport phenomena occurring at the system scale. In the cell suspension, salt concentration and temperature distributions in the cryovial or flat bag are also affecting the survivability of cells. As a specific example for this, the methodology developed to model cell suspension during cryopreservation to predict aspects of a one dimensional freezing process in a cryovial containing *NaCl* solution and equine sperm cells. The goal of this study is to calculate transient temperature and solute concentration distributions and corresponding cell responses at any location in a cell suspension during cooling processes as functions of time and distance from wall of the cryovial. Calculations for freezing of cell solution with varying initial salt concentration from 5% to 10% weight at different holding temperatures has been done.

1.2 Literature Review

In 1776 Spallanzani was the first to describe about the preservation of motility of human spermatozoa after experience to low temperature [6] and then in the year 1866 Mantagazza recommended sperm banks for frozen human semen. But the unintended discovery of glycerol as a cryoprotectant gave a new path to the field of cryopreservation [18] and till date storage of living systems using reduced temperature has been applied efficaciously to several mammalian systems which involves erythrocytes, gametes, lymphocytes, embryos, hepatocytes, bone marrow stem cells, pancreatic tissues [2], [4], mammalian oocytes [19], stem cells, rat and human liver slices and engineered tissues [5]. Its appliances are also stretched in a variety of fields such as food science, plant and animal cold hardiness, agriculture and ecology. But still there are many pros and cons that need to be considered during the low temperature freezing process which will lead towards establishing a proper cryopreservation protocol resulting in maximum cell viability. In early 1950s Lovelock suggested that increasing salt concentrations in a cell might cause damages to the cell because of cell dehydration [11]. Mazur in the year 1963 proposed that, the survival of various cells subjected to low temperature is higher when they are cooled slowly. This is due to the decrease in probability of intercellular freezing as it permits the water to leave the cell rapidly to keep protoplasm at its freezing point. He did the experiment with various mammalian cells with different cooling rates and found that at the cooling rate of $1^{\circ}\text{C}/\text{min}$ the intercellular water content is closer to the equilibrium value. Hence the amount of ice formation at this cooling rate will be less [16]. He also studied the rapidly frozen suspension of yeast cells by differential thermal analysis [20]. Bank with Mazur stated that when cells are cooled at rates exceeding a critical velocity, a decrease in viability is caused by the presence of intracellular ice. The experiment was conducted with yeast cells (*Saccharomyces cerevisiae*) and it was observed that cells cooled at a rate of $7^{\circ}\text{C}/\text{min}$ showed maximum viability.

In 1972, Mazur et al. measured that the survival of cell is related to the cooling rate and found that post-thaw viability of cells at an intermediate cooling rate is higher than that of faster and slow cooling rate where survival rate is much lower [12]. They also suggested that the injuries associated with fast and slow cooling rate are the consequences of intracellular ice formation (IIF) and excessive dehydration respectively. Muldrew and McGann proposed a hypothesis about the mechanism of intracellular ice formation which occurs due to the osmotic imbalance across the plasma membrane. An indication of this hypothesis is that mathematical models can be used to design protocols to avoid damaging gradients in osmotic pressure, allowing new approaches to preservations of cells, tissues and organs by rapid cooling [21] and later they proposed a mathematical frame work which gave an accurate description of the phenomenology of intracellular ice formation [21].

Karlsson et al. in 1994 developed a theoretical model for predicting the kinetics of ice crystallization within the cells during cryopreservation and also studied the effect of glycerol concentration on intracellular crystal growth in mouse oocytes [22]. And further study on the effect of different cryoprotective additives on intracellular ice formation (IIF) and extracellular ice formulation (EIF) was accomplished by Mazur et al. [19]. As discussed earlier these cryoprotectants act as a solvent to dilute the intracellular and extracellular solute concentrations when water is removed, thus protecting the cell from solution effects injuries and they also reduce the rate of formation ice crystals [2]. Depending on their ability to transport across cell membrane, cryoprotective agents (CPAs) are categorized into penetrating, e.g. glycerol and Dimethyl Sulphoxide (DMSO), Propylene Glycol (PG) and non-penetrating, e.g. lactose and trehalose. And the selection of CPA to be used during freezing process entirely depends upon the property (type) of the substance (cell) to be cryopreserved. Currently, glycerol and DMSO are the most commonly used CPAs because the effectiveness is much higher in their cases as compared to other CPAs for most of the substances. Usually, glycerol and DMSO are used 5 – 10% (v/v) in concentrations. Prior to being added to the cell suspension, CPAs should be diluted to the desired concentration in fresh growth media. This procedure reduces the potential toxic effects as because; presence of cryoprotectants can be hazardous when used in higher concentrations. A new era of cryopreservation was started when scientists discovered the use of differential scanning calorimeter (DSC) and Cryomicroscope. Using DSC the water transport can be measured in a cellular system during freezing. But it has some limitations, that it requires a prior knowledge about the biophysical parameters such as the initial volume, osmotically inactive cell volume and surface area, and the technique alone cannot determine whether the heat released from supercooled cellular water is due to dehydration or intracellular ice formation. Cryomicroscopy was used to address these limitations [8], [23]. Using this technique the researchers investigated the effect of cooling rate on the biophysical parameters for different cell lines and formulated the optimal cooling rate for them. Other than this, cell parameters were also studied using optical microscopy [27] and electron paramagnetic resonance method [28].

An explicit scheme for coupling temperature and concentration fields in solidification Voller 2004 models has been extensively studied. A numerical scheme for coupling temperature and concentration fields in a general solidification model is presented. A key feature of this scheme is an explicit time stepping used in solving the governing thermal and solute conservation equations [24]. This explicit approach results in a local point-by-point coupling scheme for the temperature and concentration and avoids the multi-level iteration required by implicit time stepping schemes. The proposed scheme is validated by predicting the concentration field in a benchmark solidification problem. Results compare well with an available similarity solution. The simplicity of the proposed explicit scheme allows for the incorporation of complex microscale models

into a general solidification model.

Voller and Prakash 1987 proposed a fixed grid numerical modelling methodology for convection-diffusion mushy region phase-change problems-enthalpy formulation based fixed grid methodology is developed for the numerical solution of convection-diffusion controlled mushy region phase-change problems. The basic feature of the proposed method lies in the representation of the latent heat of evolution, and of the flow in the solid-liquid mushy zone, by suitably chosen sources. There is complete freedom within the methodology for the definition of such sources so that a variety of phase-change situations can be modelled [25].

Water transport during freezing has been extensively studied by using various methods. One such method is measurement of water transport in single spherical cells by using cryomicroscopy technique [26]. Cryomicroscopy involves the application of cryogenic temperatures to cellular systems mounted under a light microscope to study the biophysical response of cells to freezing. The quantitative measurement of water transport during freezing of a tissue system were efficiently performed by using directional solidification device and two-step freezing technique [27]. A shape independent Differential Scanning Calorimeter (DSC) technique has recently been applied to measure the membrane permeability parameters in both cell and tissue systems [7], [23].

1.3 Objective

The objective of current study is as follows:

- Use the mathematical model to predict transient temperature and solute concentration distributions and corresponding cell response at any location (in the solidified, mushy, and liquid regions) in a cell suspension during cooling process as a function of time.
- Parametric calculations of freezing of a cell solution with initial salt concentration of 5% and 10% weight aqueous salt solution at different cooling conditions.
- Predictions of the kinetics of water loss, normalised volume and survivability of model cell by using the temperature profile and salt concentration data.

2.1 Overview of Solidification Phenomena

The solidification of a pure liquid, a solution, or a solution saturating a porous solid involves a complex interplay of many physical effects. The solid–liquid interface is an active free boundary on which latent heat of fusion is liberated during phase transformation. This heat is conducted away from the interface through the solid and/or liquid establishing thermal boundary layers near the interface. Further, across the interface the density changes, say, from ρ_l to ρ_s . Thus, if $\rho_l > \rho_s$, so that the material shrinks upon solidification, there is a flow induced toward the interface from “infinity.” Freezing of aqueous solutions containing solutes such as sodium chloride or glycerol is relevant to cryopreservation purposes. During freezing of such solutions pure ice is the first solid phase to form. Numerical models of the freezing process for the case of nonplanar (dendritic) freezing, where local thermodynamic equilibrium can be assumed in the entire mushy region, have allowed treatment of combined heat and mass transfer in the region. We consider a series of situations which sequentially bring out the main concepts involved in the cryopreservation as solidification of pure liquids, solutions, and cell suspended solution.

2.2 Solidification of a Pure Liquid

One of the simplest physical situations in which a liquid undergoes a phase change and transformed into a solid is as follows. The semi-infinite region $x > 0$ is a pure liquid and

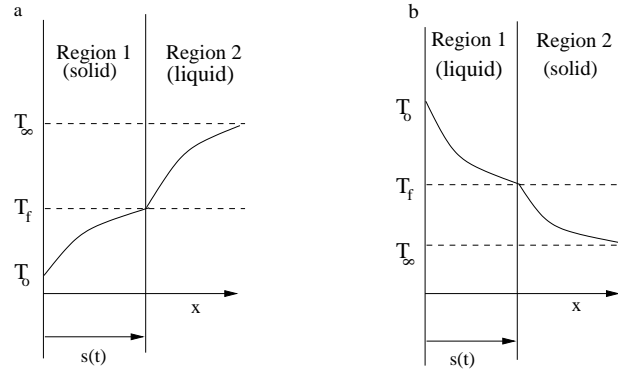


Figure 2.1: Schematic model of phase change heat transfer of a pure substance: (a) freezing and (b) thawing.

at a uniform temperature T_0 . At time $t = 0$ the temperature at the boundary of the fluid at $x = 0$ is suddenly lowered to T_b and subsequently maintained at that value, which is lower than the freezing temperature of the liquid, T_f as depicted in Fig. 2.1a. The problem is to determine the unknown, moving solidifying interface, $s(t)$, and the temperature distributions, $T(x, t)$, in both the liquid and the solid in this one-dimensional problem. If the thermophysical properties of the liquid and solid phases are assumed to be independent of temperature, the problem requires the solution of the transient heat conduction equations.

$$\rho_s c_s \frac{\partial T_s}{\partial t} = k_s \frac{\partial^2 T_s}{\partial x^2} \quad (0 < x \leq s(t)) \quad (2.1)$$

$$\rho_l c_l \frac{\partial T_l}{\partial t} = k_l \frac{\partial^2 T_l}{\partial x^2} \quad (s(t) < x) \quad (2.2)$$

Where ρ, c , and k are the density, specific heat, and thermal conductivity, respectively, with subscripts l and s denoting values in the liquid and solid, respectively. The regions occupied by the two phases are linked by the continuity of temperature at the interface,

$$T_s(s, t) = T_l(s, t) = T_f \quad (x = s(t)). \quad (2.3)$$

If the work associated with the volume change due to solidification is neglected, the continuity of the heat flux at the interface can be written as

$$\rho_s \Delta h_f \frac{ds}{dt} = k_s \frac{\partial T_s}{\partial x} - k_l \frac{\partial T_l}{\partial x} \quad (2.4)$$

Where Δh_f is the latent heat of fusion. Finally, there are boundary conditions on the temperature,

$$T = T_0 \quad x = 0 \quad (2.5)$$

and

$$T \rightarrow T_\infty \quad (x \rightarrow \infty \text{ or } t \rightarrow 0) \quad (2.6)$$

The mathematical problem described by Eqs. 2.1- 2.6 is referred to as the Stefan problem.

2.3 Freezing of a Binary Solution

Any study of solidification of a binary (e.g., water and sodium chloride) or multicomponent system must be based on the phase diagram, which specifies the possible states of liquid and solid at thermodynamic equilibrium as a function of temperature and composition. A typical phase diagram for a two-component X–Y system (at constant pressure) is illustrated in Fig. 2.2. Above the two branches of the liquidus, the system is totally liquid. Nucleation of small solid crystals occurs at a temperature below the liquidus temperature of the appropriate branch of the solidus of a solution of a given initial composition. As opposed to pure substances, liquid and solid can coexist in equilibrium over a range of temperatures up to the eutectic point. As the temperature of the solid–liquid interface is lowered, the compositions of the solid and liquid constantly change. As indicated by the solidus line in Fig. 2.2, on the left side of the eutectic point the solubility of species Y is much lower in the solid. This rejection of species causes concentration in the liquid at the interface along the liquidus line up to the eutectic composition. At the eutectic point two solid phases (α and β) of different composition form simultaneously and isothermally, such that the average composition is equal to the eutectic composition. What is important to stress is that in binary systems the phase transformation takes place over a temperature range rather than a discrete temperature as in single-component systems. As the temperature gradient is usually smaller than the equilibrium liquidus temperature gradient on the liquid state of the solid–liquid interface due to the relatively poor transfer of species compared to that of energy, the liquid in front of the growing interface is undercooled and the resulting morphological instability leads to a pattern formation. Among the most common modes of crystal growth are the dendritic patterns in which tree-like microscopic structures develop over a vol-

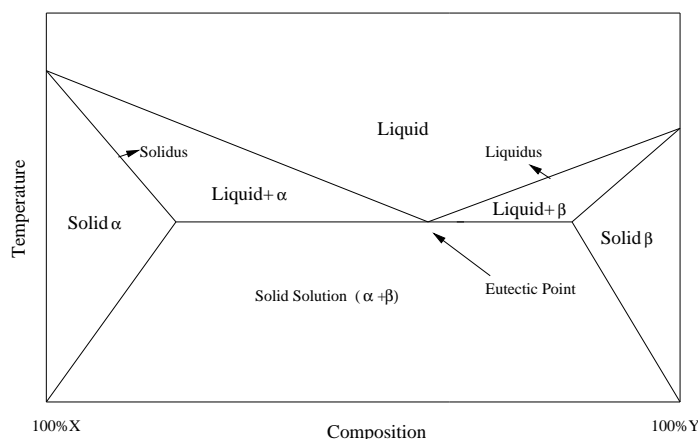


Figure 2.2: Equilibrium phase diagram for a fictitious binary system X–Y.

ume having the much larger spatial extents than the length scales of the dendritic array. The two-phase region is called the mushy zone (region).

In modeling solidification of binary and multicomponent mixtures, the complicated dendritic structures present in the mushy zone make it virtually impossible to utilize a microscopic formulation of the fundamental conservation equations and interface conditions. Therefore, the present methods of analysis are largely based on simplified (macroscopic) models of solidification and transport processes. Due to the complicated nature of the two-phase mushy zone, the models are usually based on a combination of classical conservation principles and semiempirical laws that describe the interactions between the solid and liquid phases.

Macroscopic solidification models are usually derived for a finite size averaging volume that contains both solid and liquid. This volume is much smaller than the system but much larger than the characteristic length of the interfacial structures (i.e., dendrite arms). The single domain models are based on the governing equations that apply in all (liquid, solid, and mushy) regions of the system. The equations are integrated across the entire domain without the need to explicitly subdivide the domain into solid, liquid, and mushy regions. These regions are explicitly defined within the system by distributions of energy and composition of the model equations. The single domain model equations for dendritic solidification have been based on the following approaches: (i) mixture theory, (ii) mixture-continuum model, and (iii) volume averaged model. The mixture continuum and the volume averaged models are based on virtually the same assumptions. Suffice to note that for predictions based on a stationary solid phase, results obtained from a continuum model are consistent with those based on a volume averaged model.

For solidification of biological media, as a first approximation it may be assumed that no fluid motion will occur in the melt, and the transport of both heat and chemical species is by molecular diffusion. This implies that fluid motion due to density differ-

ence between the solid and liquid phases and due to buoyancy forces can be neglected. Species diffusion in the solid phase is also neglected, and thermal and phase equilibria are assumed. In the mushy region, the temperatures of solid and liquid phases are the same and their relations to the local liquid concentration are represented by the liquidus of the equilibrium phase diagram.

Under the above assumptions the single domain energy equation for the mixture can be written as

$$\frac{\partial(\rho h)}{\partial t} = \nabla \cdot \left(\frac{k}{c_s^*} \nabla h \right) + \nabla \cdot \left[\frac{k}{c_s^*} \nabla (h_s - h) \right] \quad (2.7)$$

The dependent variable in the energy Eq is the mixture enthalpy h with $h^* = c^* T$. In this equation, ρ and k are the density and thermal conductivity of the system, respectively, and c^* is the specific heat of the solid at an arbitrary reference temperature. If temperature instead of enthalpy is used as a dependent, the Fourier–Biot law is recovered.

The species (solute) conservation equation for the mixture can be written as

$$\frac{\partial C}{\partial t} = \nabla \cdot (D \nabla C) + \nabla \cdot [D \nabla (C_1 - C)] \quad (2.8)$$

where C is the concentration and D is the diffusion coefficient. The second term on the right hand side of this equation is a diffusion like source term, which arises because mass diffusion is assumed to be significant only in the liquid phase.

The model Eqs.2.7 and 2.8 are coupled and must be used with a closure model to determine the local temperature, liquid composition, and mixture mass and volume fractions. Assuming local thermodynamic equilibrium between phases, these quantities can be found from the mixture enthalpy, h , mixture concentration, C , and an equilibrium phase diagram.

A general solidification, see Fig. 2.2, involves a spatial region over which both solid and liquid coexist as so called “mushy region.” Often the scale required for the resolution of the solid–liquid interface, in this region, is several orders smaller than the typical cell size used in a discrete numerical solution of the governing macroscopic transport equations. A powerful modeling concept in this situation is the representative volume element (REV), introduced to the solidification modeling community by Ni and Beckermann [1].

The essential part of a solidification model is the definition of a set of consistent variables that can describe the state of the solidification. Meso variables [24], These variables are uniform in the REV. If heat and liquid mass transport is relatively rapid

the meso variables are temperature T , liquid solute concentrations C_l^k , solid phase enthalpy 2.9.

$$h_s = c_s T \quad (2.9)$$

where c_s , which in general can be a function of temperature and concentration—is a specific heat term, and liquid phase enthalpy 2.10.

$$h_l = c_l T + \Delta H \quad (2.10)$$

where c_l , which in general can be a function of temperature and concentration—is a specific heat term and ΔH is the latent heat of fusion at a reference temperature, Mixture enthalpy 2.11.

$$[\rho H] = g \rho_s h_s + (1 - g) \rho_l h_l. \quad (2.11)$$

where g is the solid volume fraction in the REV.

Mixture concentration (for a given solute component, $k = 1; 2; \dots; m$)

$$[\rho C]^k = g \rho_s \langle C_s^k \rangle^s + (1 - g) \rho_l C_l^k \quad (2.12)$$

The full solution of the thermal and solute field requires additional coupling relationships. Two obvious relationships are the definitions of the mixture enthalpy $[\rho H]$, Eq. 2.11, and the mixture concentration $[\rho C]$, Eq. 2.12. Solidification of secondary phases will depend on the particular details of the phase diagram, in a binary-eutectic solution (alloy), during primary solidification the temperature and liquid concentration are related through the liquidus surface 2.13.

$$T = T_f - m C_l \quad (2.13)$$

where T_f is the fusion temperature of the pure solvent and m is the slope (assumed constant) of the liquidus line. Further the concentration in the primary α solid, at the solid-liquid interface, is $C_s = k_{par} C_l$. When the eutectic concentration is reached, however, although there is partitioning between the primary α phase and secondary β phase, there is no net solute partitioning between the combined solid phases and the liquid, and further solidification occurs isothermally at the eutectic temperature, $T = T_{eut}$.

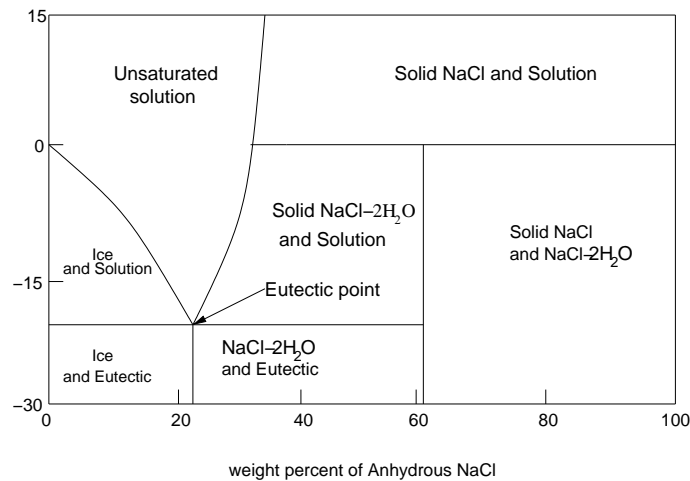


Figure 2.3: Equilibrium phase diagram of aqueous sodium chloride solution [1].

2.4 Freezing of water sodium chloride solution

As an application of the analyses that have been developed for calculating the solidification of binary solutions, we consider the freezing of $H_2O-NaCl$ solution which is common solution for the freezing of a cell suspension. The equilibrium diagram for the solution is given in Fig. 2.3. The specific objective is to calculate the transient temperature and solute concentration distributions in the frozen, mushy zone, and melt regions and then use the data to calculate cell response (membrane transport, water flux, and cell volume change) to the thermal and solute concentration changes.

2.5 Mathematical Model of Water Transport

A mathematical model has been developed by Mazur [28] for predicting the volumetric change in cells due to the loss of intracellular water across the cell membrane during a freezing process in the presence of extra cellular ice. Mazur's water transport model was later modified by Levin et al [29], by presuming the permeability of the membrane depends on the temperature. Water transport model assumes an idealized biological cell as an open thermodynamic system having a semi-permeable membrane boundary. The model also assumes: 1) infinite extracellular space while the cellular space is the volume of sphere ($V = 4\pi r^3/3$); 2) the cellular space is the volume of the geometry of the cell being studied; 3) effective membrane surface area available for water transport ($A_c = 4\pi r_0^2$) is constant based on the original cell radius, r_0 [15]; 4) the intracellular solution is ideal and dilute [30]; 5) the temperature differentials across the cell membrane are negligible; and 6) the latent heat of water is constant ($335\text{mJ}/\text{mg}$) in the temperature range of interest [20]; 6) the hydrostatic pressure difference across the cell plasma membrane is zero (a good assumption for mammalian cells). The plasma membrane permeability is

assumed to be temperature dependent and is represented by an Arrhenius relationship as given by Levin et al [29] and shown in Eq. 2.20. In its simplest form water transport model can be represented as,

$$\frac{dV}{dT} = - \frac{L_p A_c R T}{B v_w} \left(\ln \frac{a_i^w}{a_o^w} \right) \quad (2.14)$$

where V is the cell volume, T is the absolute temperature, L_p is the permeability of the membrane to water, R is the gas constant, B is the constant cooling rate, A_c is the effective membrane surface area available for water transport, v_w is the partial molar volume of water, and a_i^w is the chemical potential of the intracellular fluid and a_o^w is the chemical potential of extracellular fluid. Quantitative use of the above thermodynamic model requires a more complete specification of the chemical activities of the extracellular and the intracellular solutions, along with the membrane water permeability.

The extracellular solution is assumed to be composed of a binary solution consisting of water and sodium chloride and can be modeled using the equilibrium properties of a solid/liquid solution. The Gibbs-Helmholtz equation relates the equilibrium water activity in the solution as a function of temperature as,

$$\frac{\partial (\ln a_w)}{\partial T} = \frac{\Delta H_f}{RT^2} \quad (2.15)$$

where ΔH_f is the latent heat of fusion of water, which is assumed to be constant in the temperature range of interest (0 to $-45^\circ C$) as 335 mJ/mg . Integrating the above expression yields the extracellular activity as,

$$\ln a_w = \frac{\Delta H_f}{R} \left[\frac{1}{T_R} - \frac{1}{T} \right] \quad (2.16)$$

where T_R is the reference temperature (273.15 K). The intracellular solution is typically modeled as an ideal and dilute solution so that the chemical activity of the internal water is equal to the mole fraction of the water,

$$a_w^i = X_w^i \quad (2.17)$$

Neglecting the cell membrane volume and recognizing that some of the intracellular fluid may be bound water, that is water which is not free to move across the cell membrane in response to an osmotic gradient (which is included in the osmotically inactive cell volume V_b), the mole fraction of intracellular water is given as,

$$X_w^i = \frac{V - V_b}{(V - V_b) + \varphi_s n_s v_s} \quad (2.18)$$

where φ_s is the disassociation constant for sodium chloride, n_s is the number of moles of solutes in the cell as calculated from initial cell osmolarity and the total osmotically active cell water volume ($V_o - V_b$) where V_o is the initial isotonic cell volume and, V_b is the osmotically inactive cell volume. Substituting Eqs. 2.16 and 2.18 in Eq. 2.14, one arrives at the Mazur model of water transport,

$$\frac{dV}{dT} = - \frac{L_p A R T}{B v_w} \left[\ln \frac{(V - V_b)}{(V - V_b) + v_w (v_s \varphi_s)} - \frac{\Delta H_f}{R} \left[\frac{1}{T_R} - \frac{1}{T} \right] \right] \quad (2.19)$$

The temperature dependence of the membrane permeability to water (L_p) is expressed as an Arrhenius relationship (Levin et al 1976) [29],

$$L_p = L_{pg} \exp \left[-\frac{E_{Lp}}{R} \left(\frac{1}{T} - \frac{1}{T_R} \right) \right] \quad (2.20)$$

where L_{pg} is the permeability of the membrane to water at a reference temperature ($T_R = 273.15K$) and E_{Lp} is the apparent activation energy for the permeability process.

In this study, the equine sperm is modeled as a long cylinder with length $L = 36.5\mu m$ and a radius $r_o = 0.66\mu m$, which translates to $V_o \sim 50\mu m^3$ and $A_c \sim 150\mu m^2$. The osmotically inactive cell volume (V_b) was assumed to be $0.6V_o$, a value within the range reported for a variety of mammalian sperm [8], [18]; R is the universal gas constant ($8.314J/molK$); B is the constant cooling rate (K/min); v_w is the molar volume of water ($18 \times 10^{12}\mu m^3/mol$); φ_s is the disassociation constant for salt(2); n_s is the number of moles of salt, $C_i \cdot (V_o - V_b)$, where C_i is the initial cell osmolality ($0.285 M$); ΔH_f is the latent heat of fusion of water ($335mJ/mg$); and ρ is the density of water ($1000kg/m^3$).

As stated earlier in the introduction, cooling rates that are either "too high" or "too low" can reduce the post thaw survival of the cells either by "intracellular ice formation" or by "solute damage" respectively [12]. Based upon this two factor hypothesis of freezing injury, a cooling rate for maximum cell cryosurvival should and does exist between the "high" and "low" rates [3]. This has been confirmed analytically for equine sperm cells and the curve of cell survival plotted as a function of the cooling temperature.

Whether a cooling rate is "too high" or "too low" for a given cell type depends on the location and on the various cell parameters including L_{pg} , E_{Lp} , V_b , V_o , and the available cell membrane surface area (SA). The last three parameters (V_b , V_o , SA) can be collapsed into a single parameter, SA/WV (by defining WV as the initial intracellular water volume or $WV = V_o - V_b$). Following Mazur [31] and others [7] [8], defined the optimal cooling

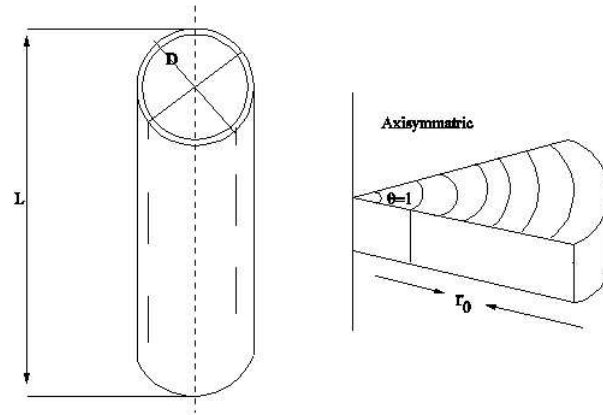


Figure 2.4: Schematic diagram of cryovial and coordinate system.

rate as the “highest” cooling rate which traps 5% of the initial intracellular water (WV) at an end temperatures. In this study, the cooling rate profiles are not mentioned but places, where the cell influenced whether high or slow cooling rate are predicted.

2.6 Numerical Simulations

A cryovial containing the cell suspension is idealized as a symmetric, one-dimensional region of thickness L and radius r (Fig.2.4). The temperature of the outside boundaries is assumed to vary with time. Initially the solute concentration is uniform; volume change during solidification is negligible; the solution does not supercool and the thermophysical properties of the melt and solid are independent of temperature and concentration. If buoyancy forces are neglected and there is no flow induced by the density change during freezing, the solution will remain stagnant and the model described by Eqs.2.7 and 2.8 will be applicable. The equilibrium phase diagram of aqueous sodium chloride solution given by Song et al [1], was used to close the model (Fig. 2.3). A numerical method of solution was employed to solve the one-dimensional (Cylindrical geometry) form of model Eqs. 2.7 and 2.8. The mass-averaged specific heat and the volume averaged effective thermal conductivity are used in the calculations. The initial and boundary conditions for the transport equations are

$$T = T_i, \quad C = C_i \quad \text{at } t = 0, 0 < x < L,$$

$$\frac{\partial T}{\partial x} = \frac{\partial C}{\partial x} = 0 \quad \text{at } x = L,$$

and

$$T = \frac{\partial C}{\partial x} T_i + At, \frac{\partial C}{\partial x} = 0 \text{ at } x = 0,$$

where A is a cooling temperature at the outside surface of the cryovial wall.

The energy and solute conservation equations were discretised utilizing the control volume formulation and a fully implicit scheme. The numerical procedure for solving the finite-difference equations was similar to that developed by Prakash and Voller [25]. The main difficulties encountered were in dealing with equations representing the equilibrium phase diagram of $H_2O-NaCl$. The locations of liquidus and solidus are not known a priori, and an iterative procedure is necessary at each time step (34). At each iteration the discretized model conservation equations are solved for the mixture enthalpy (h) and the solute concentration (C). Then, the fraction of the liquid phase and the fraction of the eutectic solid are determined [32]. Analytical predictions are compared with experimental data published by Barga and Viskanta [33] to establish the validity of the analytical model.

Freezing of $H_2O-NaCl$ solution was simulated for the following values of the model parameters:

- Solution layer thickness: 5 mm
- Cryovial material: Polyethylene.
- Cryovial material thickness: 0.5 mm
- Initial NaCl salt concentrations: 5% and 10% weight
- Cell density: $10^{12} \text{ cells}/\text{m}^3$
- Initial temperatures: $-20 \text{ to } -50^\circ\text{C}$.

The freezing protocol starts with a constant heat being imposed on the outer boundary of cryovial Fig 2.4, when the freezing temperature is reached at this boundary, ice appears and begins to propagate through cell and solution inside the cryovial. As the cells express water in response to upset in thermodynamic equilibrium, they shrink and engulfed by the advancing solid phase.

the overall solution of the problem will be a two step process. First, the temperature and concentration will be determined for the freezing process. These fields determined for the freezing of $H_2O-NaCl$ solution at various concentration. The Final step is to determine the thermodynamic states corresponding to these temperature and concentration fields. The departure of these states from equilibrium will determine the kinetics of cellular water transport by use of Levin [29] model.

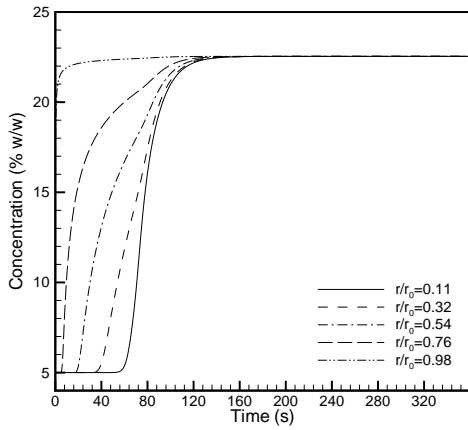
The conservation equations for transient temperature and concentration and water transport equation shown above (2.7 and 2.8) was numerically solved by CFD using a method to calculate the optimal cooling temperature values and cell survivability over a wide range of various cell level parameters. A numerical FORTRAN code was developed and simulations were performed on HP workstations in the Fedora environment. The key parameters chosen for this parametric investigation are, permeability of the membrane to water (L_{pg}), apparent activation energy (E_{Lp}), inactive cell volume (V_b), diameter (D), end temperature (T_{end}), and the ratio of the available surface area for water transport to the initial volume of intracellular water (SA/WV).

Results & Discussion

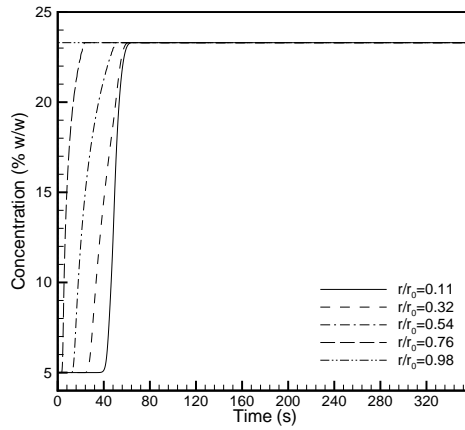
The calculation is carried out for 5% and 10% weight aqueous salt solution. The solution is stored in a constant temperature bath having temperatures of $-20^{\circ}C$, $-30^{\circ}C$, $-40^{\circ}C$, and $-50^{\circ}C$. The cell being cryopreserved is equine sperm which has following biophysical properties: isotonic cell volume $V_0 = 50\mu m^3$, inactive cell volume $V_b = 0.6V_0$, cell surface area $SA = 150\mu m^2$, membrane permeability $L_{pg} = 0.02\mu m/(min-atm)$, and activation energy $E_{lp} = 32.7Kcal/mol$. The temperature distribution, salt concentration, and cell response are plotted in the following sections. It should be noted that the different cooling rate inside the solution results in nonuniform dehydration of cells, which in turn affects survivability. Therefore, survivability is also presented for the studied cases.

3.1 Temperature and Concentration distribution in cryovial

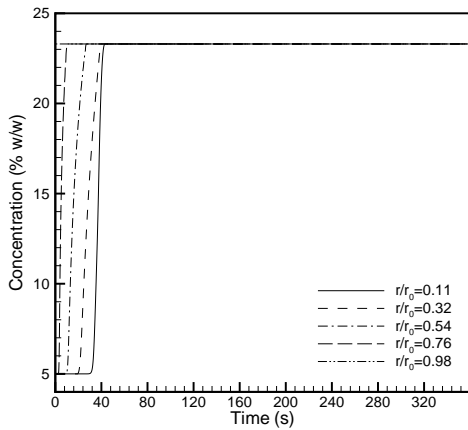
The salt concentration distributions in the cryovial with time as a parameter are illustrated in Figures 3.1 and 3.3. As the solution freezes, salt is rejected in the mushy zone, the salt concentration increases very sharply, and a very thin concentration boundary layer is formed ahead of the solidus front. Fig 3.1, the salt concentration in the liquid varies from 5% in the liquid region up to the eutectic concentration (23.3%) at the solidus interface. For instance, 22s after the concentration has increased to approximately 6% at $r/r_0 = 0.54$. At 60s, there is solid present across more than half of the solution thickness, but no eutectic transformation has occurred, since the maximum salt concentration in the mushy zone is equal to 17%. Whole of the binary solution is converted into eutectic solid at time instances of 130s, 60s, 45s and 38s for the case when initial cooling



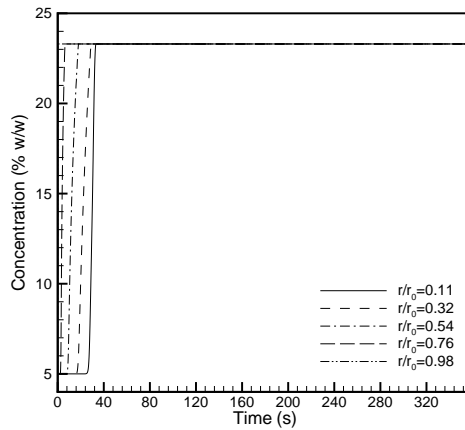
(a) During holding temperature -20°C .



(b) During holding temperature -30°C .



(c) During holding temperature -40°C .



(d) During holding temperature -50°C .

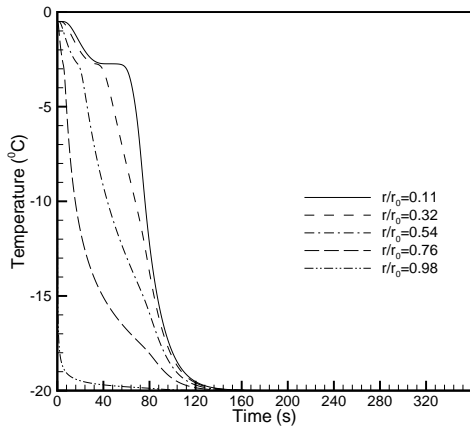
Figure 3.1: Solute concentration distribution in the solution during freezing of 5% weight at a different cooling conditions.

temperature is -20°C , -30°C , -40°C , and -50°C respectively. Note the high salt concentrations, varying from 17% at the center of the vial ($r/r_0 = 0.11$) to 23% to the solidus interface ($r/r_0 = 0.98$). The sharp increase in the concentration of the liquid near the vial wall is expected, since this is the location where the crystals first nucleate. Solute redistribution occurs at this location, and the ice formation drives the concentration increases up to eutectic transformation .

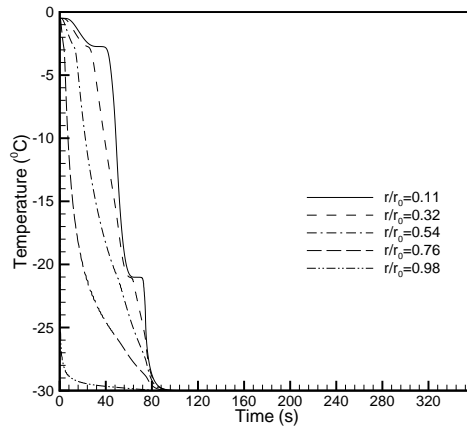
The temperature and solute concentration variations with time at a few selected locations in the vial cooled at -20°C , -30°C , -40°C , and -50°C , for varying initial solute concentrations, are illustrated in Figs. 3.1, 3.2, 3.3 and 3.4 respectively. The profiles show that after the liquidus temperature ($\sim -1^{\circ}\text{C}$) has been reached, the temperature of the solution remains nearly constant for a relatively long period of time before it starts decreasing rapidly. Near the Vial wall, the temperature gradient is larger while the solution at different locations is still liquid. Owing to the latent heat release during freezing, the temperature gradient becomes smaller, increasing significantly again only when the eutectic transformation occurs. The temperature at the two intermediate locations ($r/r_0 = 0.32$ and 0.76) reveal a similar behaviour. The time elapsed from the arrival of the dendrite tips and the eutectic transformation is much smaller than for the other locations. Temperature and concentration profiles for 10% initial solute concentration are also express similar consequences as 5% solute concentration but varies in times. Figures 3.1 and 3.3 shows the concentration profiles for the same locations as illustrated in previous concentration distributed profiles. The concentration increases due to solute redistribution for ($r/r_0 = 0.32$ and 0.76) are similar, although there is a sharp increase in concentration prior to the eutectic transformation for the second location. The third location experiences a similar profile, but the abrupt change in slope for the concentration change occurs earlier. The salt concentration at the center of the vial ($r/r_0 = 0.98$) reveals a very different profile, since the concentration change is accelerated. The consequences of these changes in the slope for cryopreservation are drastic, since the transport of water across the cell membrane is governed by the concentration differences. For different locations of the cell in the vial, different amounts of water leave the cell, affecting the survival rate of the cells in the vial.

From the figures 3.1 to 3.4, it is clear that with an increase in the salt concentration in the solution, the rate of growth of mushy zone decrease. As expected, a decrease in the wall temperature increased the freezing rate. It can be also verified that the initial temperature affects the growth of the two-phase region in the same way as the concentration. From temperature profiles, Note that the slope of the curves varies at the boundary and central locations of the cryovial at different times. These are due to changes in the phase of solution and eutectic formation. Cells express different responses in these locations, affecting the survival rate.

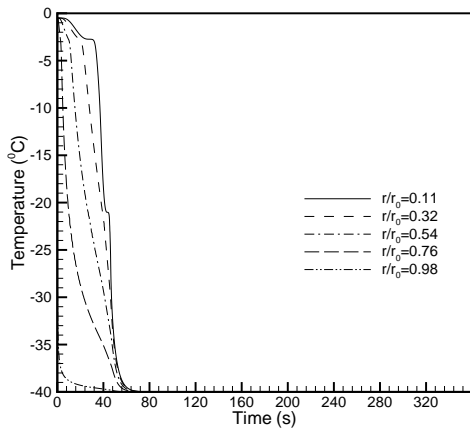
From Figs 3.1 to 3.4, the following facts are apparent: (i) kinetics of phase change



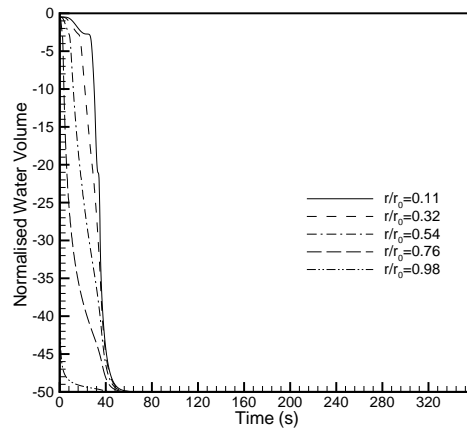
(a) During holding temperature -20°C .



(b) During holding temperature -30°C .



(c) During holding temperature -40°C .



(d) During holding temperature -50°C .

Figure 3.2: Temperature profiles in the solution during freezing of 5% weight at a different cooling conditions.

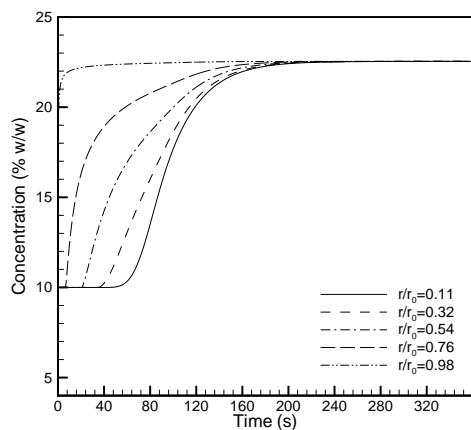
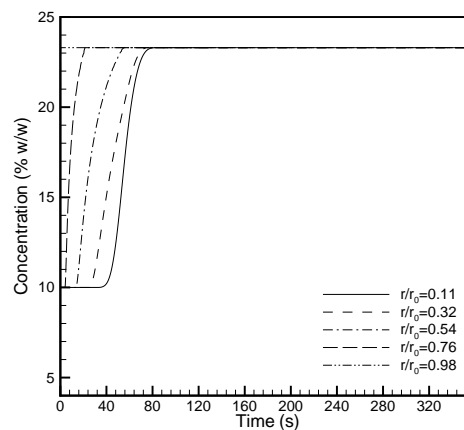
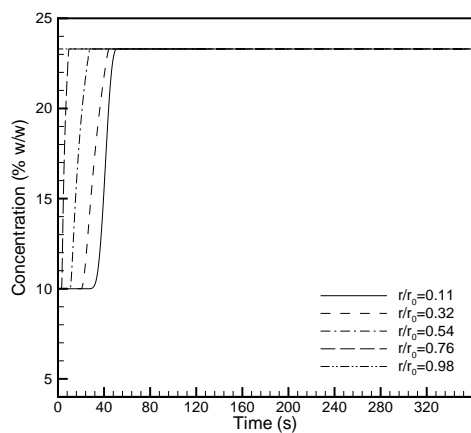
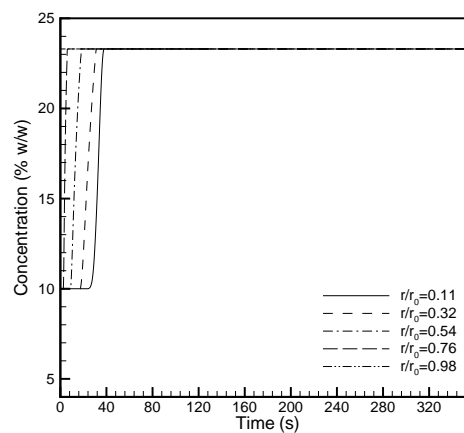
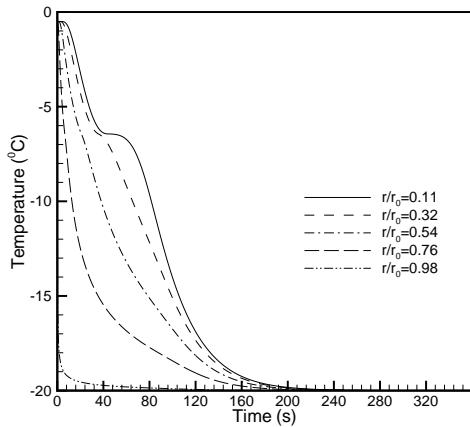
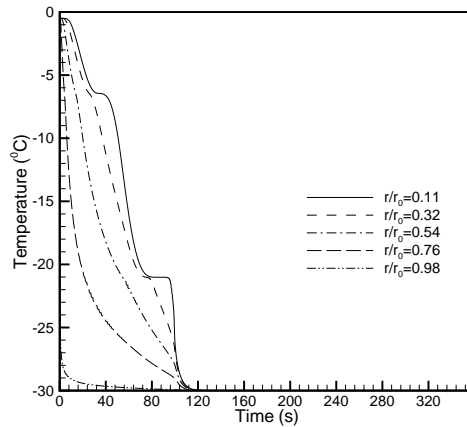
(a) During holding temperature -20°C .(b) During holding temperature -30°C .(c) During holding temperature -40°C .(d) During constant holding -50°C .

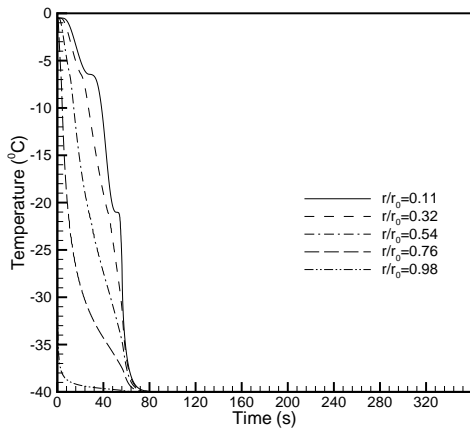
Figure 3.3: Solute concentration distribution in the solution during freezing of 10% weight of a different cooling conditions.



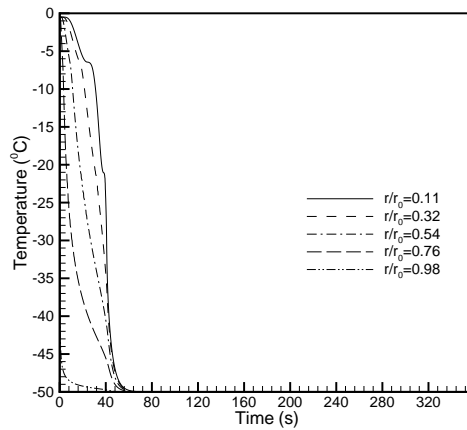
(a) During holding temperature -20°C .



(b) During holding temperature -30°C .



(c) During holding temperature -40°C .



(d) During holding temperature -50°C .

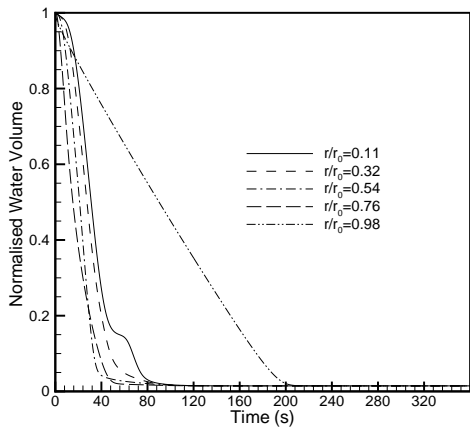
Figure 3.4: Temperature profiles in the solution during freezing of 10% weight at a different cooling conditions.

in $H_2O-NaCl$ solution is greatly influenced by the holding temperature; (ii) for a given time there are nonuniform temperature and solute concentration distributions during the cooling process; and (iii) although the temperature near vial (holding temperature) is constant, the temperature change in the sample is not a linear function of time and depends on the location. In other words, the cooling rate in one position in the solution is not constant and is different from the cooling rate at any other location. If there are cells suspended in the solution, cells at different locations will experience different cooling conditions, as discussed in the introduction. Cooling rate is a dominant factor affecting intracellular water loss, water flux across cell membrane, as well as probability of intracellular ice formation, all of which are related to the cell cryoinjury. Effect of the different holding temperature on the response of a model cell is discussed below.

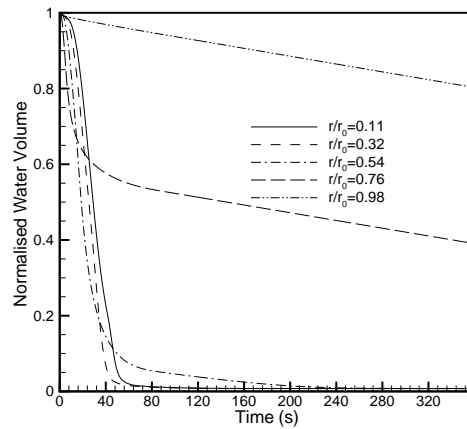
3.2 Kinetics of Cell Water Loss at Different Locations in the Cryovial

It is generally accepted that intracellular ice formation (IIF) and severe cell shrinkage, both of which are related to cell water loss, may damage cells [6], [30], [31]. Intracellular water loss of model cells, placed at various locations in the cryovial under different cooling conditions, is calculated using the Mazur equations 2.19. The calculated temperature and solute concentration distributions in the cryovial are used as local, extracellular environmental conditions for different cooling processes.

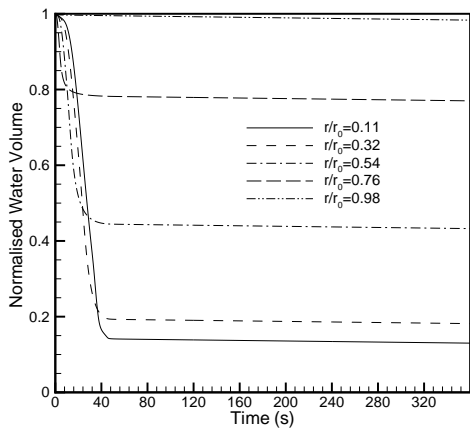
The results for the holding temperature of $-20^{\circ}C$ to $-50^{\circ}C$ for two solute concentrations of 5% and 10% are illustrated in Figs. 3.5 and 3.6. From these figures, it is found that because of the different local cooling rates, kinetics of cell water loss is different among various locations. The results in Fig. 3.5a and 3.6a show that for a fixed local temperature ($-20^{\circ}C$), intracellular water volume and the degree of supercooling are independent of cell location in the cryovial. In contrast, at a relatively higher hold temperature ($-50^{\circ}C$) (as shown in Figs. 3.5d and 3.6d), intracellular water volume and supercooling degree depend significantly on the location and is found to be much greater for those under the low cooling condition. Because of the high degree of supercooling and large intracellular water amount, ice formation will occur inside the cells during the cooling process [34], [20]. The IIF can damage the cells. However, the main purpose of the present analysis is to demonstrate, as shown in Figs. 3.5 and 3.6, that cell water loss is a function of location for any given time or any given temperature before the IIF occurs. Ice growth is a rapid process, but transport of water through the cell membrane is relatively slow, because the membrane acts as a resistance barrier. Therefore, as cooling and extracellular ice growth continue, the liquid water of the unfrozen fraction remains very close to equilibrium with the ice, but the intracellular water lags behind, consequences of these situa-



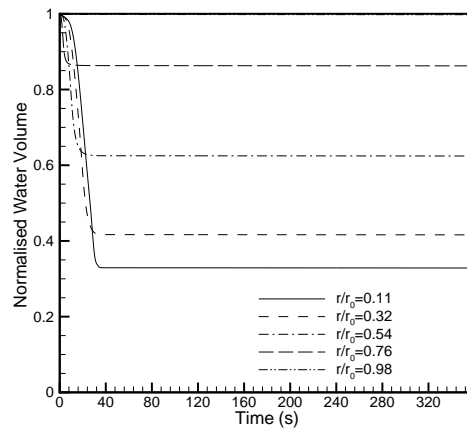
(a) During holding temperature $-20^{\circ}C$.



(b) During holding temperature $-30^{\circ}C$.



(c) During holding temperature $-40^{\circ}C$.



(d) During holding temperature $-50^{\circ}C$.

Figure 3.5: Intracellular water volume variation with time during freezing of model cells at different locations in the cryovial under boundary cooling conditions and solute concentration 5%.

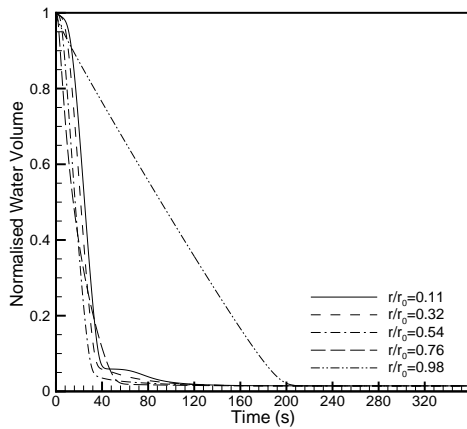
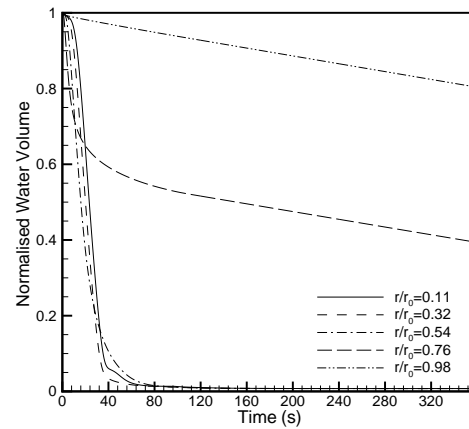
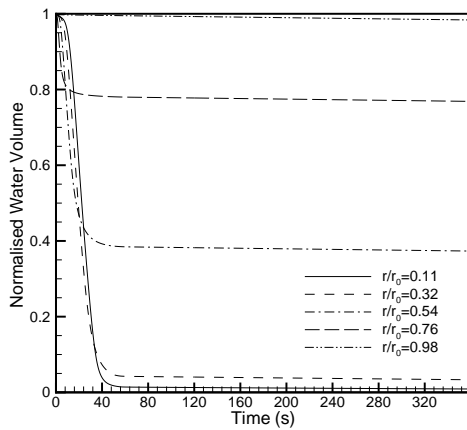
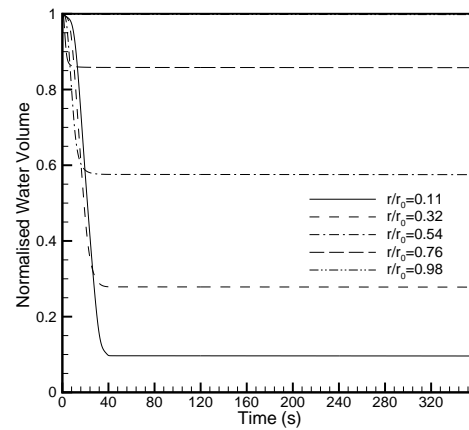
(a) During holding temperature -20°C .(b) During holding temperature -30°C .(c) During holding temperature -40°C .(d) During holding temperature -50°C .

Figure 3.6: Intracellular water volume variation with time during freezing of model cells at different locations in the crovial under boundary cooling conditions and solute concentration 10%.

tions are shown in Fig. 3.5a and 3.6a at the central location of the vial (here cell expressed slow cooling rate). After time 200s, volume of all cells decreased to zero in all locations near the boundary and centre of the vials. This means that the water concentration (i.e. the chemical potential of water) is too high for thermodynamic equilibrium, and there may be a risk of intracellular ice formation. However, when cooling rates are high in the location near to the wall of the vial, the dehydration may not be fast enough to prevent intracellular ice nucleation, then the water content inside the cells is more. Eventually, the cell volume shrinks to nearly 17% of its original volume after time 40s at $r/r_0 = 0.11$ and in the location $r/r_0 = 0.98$ cell volume shrinks to nearly 80% of its original volume after time 20s. After that the volume remains constant as shown in Fig. 3.5c. The cell volume shrinks to nearly ~ 35% of its original volume after time ~ 40s at $r/r_0 = 0.11$ and in the location $r/r_0 = 0.98$, the cell volume shrinks to nearly 90% of its original volume after time 20s. After that the volume remains constant as shown in Fig. 3.5d. Fig 3.6 shows the normalised cell volume profiles with time at the same locations as discussed previously. It shows similar cell responses in all locations, but at different time(s) and express different cell volume due to an increase in the solution concentration.

3.3 Survivability

The results of normalised cell volume variations with time at different locations during cooling process are illustrated in Figs.3.5 and 3.6. From these Figures, it can be noticed that cell volume change depends on the locations. As observed, the cells influenced different cooling rates in different locations in the cryovial. The result of viability of cells is illustrated in Fig. 3.7. It can be seen that the maximum viability of equine sperm is observed at a temperature of -38°C (i.e., 13% of control) with initial solute concentration of 5%. The results are different for holding temperatures, higher and lower than -38°C . Indeed, the cells viability fell to a point of 0% for a cooling temperature of -22°C and -42°C due to solution injury and freezing injury. While increasing the initial solute concentration up to 10%, the viability of equine sperm cells varied; it is maximum at a hold temperature of -25°C (i.e., 8% of control). The cells viability fell to a point of 6% for a cooling temperature of -43°C and then remained decreasing while increasing temperature from -43°C .

The results illustrate that the hold temperature and initial solute concentrations strongly influence cell viability. From general point of view, in each case maximum cell viability value was obtained for intermediate cooling temperatures (i.e., between -25 to -38°C). Lower cooling temperatures and very high cooling temperatures are detrimental for the cells.

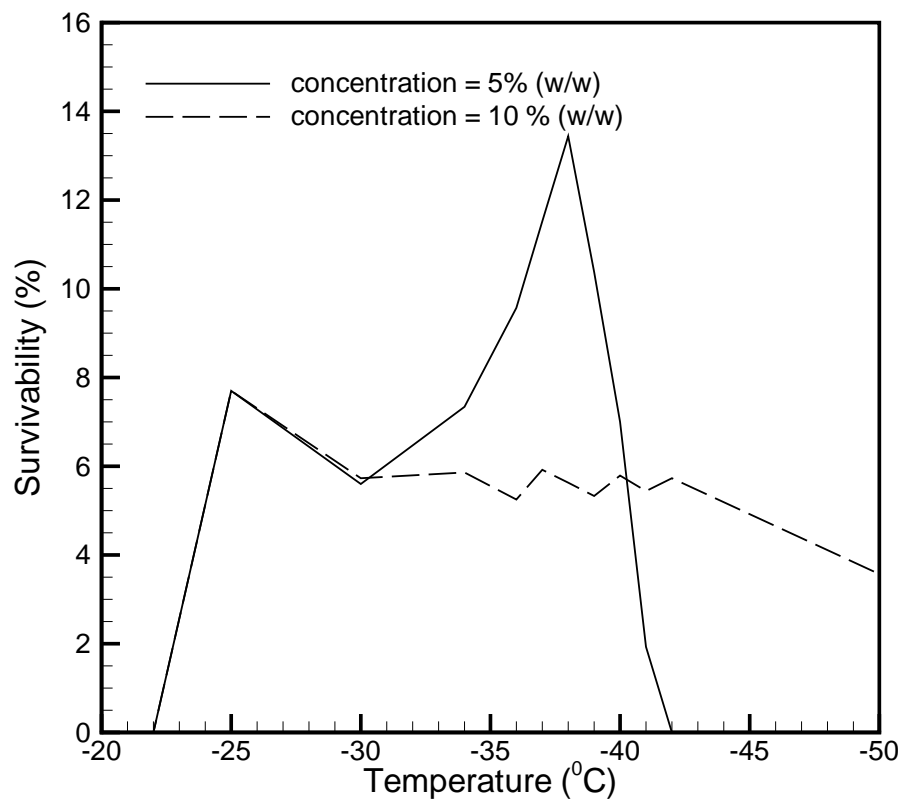


Figure 3.7: Relation of cell viability to cooling temperatures with initial solution concentrations 5% and 10%

3.4 Conclusion

In the present investigation, mathematical modeling of heat and mass transfer in a multicomponent solution and its relevance to development of optimum cryopreservation procedures are studied. By using the temperature and salt concentration data, the kinetics of water loss, normalised cell volume and survivability of model cell are predicted. The volumetric shrinkage during freezing of equine sperm suspensions at holding temperature between -20°C and -50°C in the absence of cryoprotective agents (CPAs) for different initial solute concentrations of 5% and 10% is predicted. The percentage of viable equine sperm was 13% and 8% at holding temperature of -38°C and -25°C for initial solute concentration of 5% and 10% respectively. Sperm viability is found to be almost constant between -25°C and -40°C for an initial solute concentration of 10%.

Bibliography

- [1] M. Song, J. Choi, R. Viskanta, Upward solidification of a binary solution saturated porous medium, *International Journal of Heat and Mass Transfer* 36 (15) (1993) 3687–3695.
- [2] P. Mazur, Freezing of living cells: mechanisms and implications, *The American journal of physiology* 247 (3 Pt 1) (1984) C125–142.
- [3] J. J. McGrath, K. Diller, *Low temperature biotechnology: Emerging applications and engineering contributions*, vol. 10, ASME Press, 2 edn., 1988.
- [4] A. Bernard, B. J. Fuller, Cryopreservation of human Oocytes: a review of current problems and perspectives, *Human Reproduction Update* 2 (3) (1996) 193–207.
- [5] T. R. Oegema, L. B. Deloria, A simple cryopreservation method for the maintenance of cell viability and mechanical integrity of cultured cartilage analog, *Cryobiology* 40 (10) (1999) 370–375.
- [6] S. H. Day, D. A. Nicoll-Griffith, Cryopreservation of rat and human liver slices by rapid freezing., *Cryobiology* 38 (8) (1999) 154–159.
- [7] R. V. Devireddy, D. Raha, J. C. Bischof, Measurement of water transport during freezing in cell suspensions using a differential scanning calorimeter, *Cryobiology* 36 (2) (1998) 124–155.
- [8] R. V. Devireddy, D. J. Swanlund, T. Olin, W. Vincente, M. H. T. Troedsson, J. C. Bischof, K. P. Roberts, Cryopreservation of equine sperm: optimal cooling rates in the presence and absence of cryoprotective agents determined using differential scanning calorimetry, *Biology of reproduction* 66 (1) (2002) 222–231.

- [9] P. Mazur, Cryobiology: the freezing of biological systems, *Science (New York, N.Y.)* 168 (3934) (1970) 939–949.
- [10] Mazur. P, Kinetics of water loss from cells at subzero temperatures and the likelihood of intracellular freezing, *Journal of General Physiology* 47 (5) (1963) 347–369.
- [11] J. E. Lovelock, Haemolysis of human red blood cells by freezing and thawing, *Biochimica et Biophysica Acta* 10 (5) (1953) 414–426.
- [12] P. Mazur, S. P. Leibo, E. H. Chu, A two-factor hypothesis of freezing injury. Evidence from Chinese hamster tissue-culture cells, *Experimental cell research* 71 (2) (1972) 345–355.
- [13] H. Ishiguro, B. Rubinsky, Mechanical interaction between ice crystals and red blood cells during directional solidification, *Cryobiology* 31 (8) (1994) 483–500.
- [14] H. Udaykumar, L. Mao, Sharp-interface simulation of dendritic solidification of solutions, *International Journal of Heat and Mass Transfer* 45 (24) (2002) 4793–4808.
- [15] M. Toner, E. G. Cravalho, Thermodynamics and kinetics of intracellular ice formation during freezing of biological cells, *Journal of Applied Physics* 10 (2) (1991) 463–465.
- [16] P. Mazur, Kinetics of Water Loss from Cells at Subzero Temperatures and the Likelihood of Intracellular Freezing, *The Journal of General Physiology* 47 (2) (1963) 347–369.
- [17] Viskanta, Bianchi, Critser, Gao, Solidification Processes of Solutions, *Cryobiology* 34 (4) (1997) 348–362.
- [18] C. Polge, A. Smith, Revival of spermatozoa after vitrification and dehydration at low temperatures, *Nature* 13 (3) (1949) 164–666.
- [19] P. Mazur, S. Seki, I. L. Pinn, F. W. Kleinhans, K. Edashige, Extra- and intracellular ice formation in mouse oocytes, *Cryobiology* 51 (1) (2005) 29–53.
- [20] P. Mazur, Studies on Rapidly Frozen Suspensions of Yeast Cells by Differential Thermal Analysis and Conductometry, *Biophysical Journal* 3 (4) (1963) 323–353.
- [21] K. Muldrew, L. McGann, The Osmotic rupture hypothesis of Intracellular Freezing Injury., *Biophysical journal* 66 (4) (1994) 532–541.
- [22] J. O. Karlsson, E. G. Cravalho, M. Toner, A model of diffusion-limited ice growth inside biological cells during freezing, *Journal of Applied Physics* 75 (20) (1994) 4442–4455.

-
- [23] R. V. Devireddy, D. J. Swanlund, K. P. Roberts, J. C. Bischof, Subzero water permeability parameters of mouse spermatozoa in the presence of extracellular ice and cryoprotective agents, *Biology of reproduction* 61 (3) (1999) 764–775.
- [24] V. Voller, A. Mouchmov, M. Cross, An explicit scheme for coupling temperature and concentration fields in solidification models, *Applied Mathematical Modelling* 28 (1) (2004) 79–94.
- [25] V. Voller, C. Prakash, A fixed grid numerical modelling methodology for convection-diffusion mushy region phase-change problems, *International Journal of Heat and Mass Transfer* 30 (8) (1987) 1709–1719.
- [26] K. R. Diller, E. G. Cravalho, A cryomicroscopy for the study of freezing and thawing process in biological systems, *Cryobiology* 7 (5) (1970) 191–199.
- [27] P. V. Pazhayannur, J. C. Bischof, Measurement and simulation of water transport during freezing in mammalian liver tissue, *ASME Journal of Biomechanical Engineering* 119 (10) (1997) 269–277.
- [28] P. Mazur, Studies on rapidly frozen suspensions of yeast cells by differential thermal analysis and conductometry, *Biophysical journal* 3 (9) (1963) 323–353.
- [29] Levin. R. L, E. G. Cavalho, C. Huggins, A membrane model describing the effect of temperature on water conductivity of erythrocyte membranes at subzero temperatures, *Cryobiology* 13 (6) (1976) 415–429.
- [30] G. A. Mansoori, Kinetics of water loss from cells at subzero centigrade temperatures, *Cryobiology* 12 (4) (1975) 34–35.
- [31] P. Mazur, Equilibrium, quasi-equilibrium, and nonequilibrium freezing of mammalian embryos, *Cell biophysics* 17 (1) (1990) 53–92.
- [32] S. Thirumala, R. V. Devireddy, A simplified procedure to determine the optimal rate of freezing biological systems, *Journal of biomechanical engineering* 127 (2) (2005) 295–300.
- [33] S. Braga, R. Viskanta, Solidification of a binary solution on a cold isothermal surface, *International Journal of Heat and Mass Transfer* 33 (4) (1990) 745–754.
- [34] P. Mazur, A biologist's view of the relevance of thermodynamics and physical chemistry to cryobiology, *Cryobiology* 60 (1) (2010) 4–10.